

Pion production in dAu collisions at RHIC energy

P. Lévai^{1,2,a}, G. Papp³, G.G. Barnaföldi^{1,4}, and G. Fai⁴

¹ RMKI Research Institute for Particle and Nuclear Physics, PO Box 49, Budapest, 1525, Hungary

² Department of Physics, Columbia University, 538 West 120th Street, New York, NY 10027, USA

³ Department for Theoretical Physics, Eötvös University, Pázmány P. 1/A, Budapest 1117, Hungary

⁴ Center for Nuclear Research, Department of Physics, Kent State University, Kent, OH 44242

Abstract. We present our results on neutral pion (π^0) production in pp and dAu collisions at RHIC energy. Pion spectra are calculated in a next-to-leading order (NLO) perturbative QCD-based model. The model includes the transverse component of the initial parton distribution (“intrinsic k_T ”). We compare our results to the available experimental data from RHIC, and fit the data with high precision. The calculation tuned this way is repeated for the dAu collision, and used to investigate the interplay of shadowing and multiple scattering at RHIC. The centrality dependence of the nuclear modification factor shows a measurable difference between different shadowing parameterizations.

1 Prologue

With this paper we would like to pay tribute to József Zimányi (Jozsó) who passed away in September 2006. Jozsó was an enthusiastic supporter of the Hungarian participation in the relativistic heavy ion program at the Relativistic Heavy Ion Collider (RHIC) at Brookhaven National Laboratory. He had a detailed vision about quark-gluon plasma formation at RHIC, and he was eager to confront the real world of experimental data with his ideas. In the last decade of the construction phase of RHIC he predicted many observables, including hadron numbers and ratios [1]. He realized that the era of high- p_T physics and QCD is coming to nuclear physics, because the RHIC detectors extended the measurable transverse momentum region much beyond the SPS values of $p_T = 3 - 4$ GeV/c. He followed the progress in this subfield and was always happy to discuss related questions.

Jozsó joined the Hungarian experimental PHENIX group from its foundation and supported continuously the Hungarian activity by full heart and by his authority. The first PHENIX paper on which his name appears is entitled “*Absence of suppression in particle production at large transverse momentum in $\sqrt{s_{NN}} = 200$ GeV in $d + Au$ collisions*” [2], and has become a fundamental reference in the quest for understanding hadron suppression and jet energy loss in deconfined matter in $AuAu$ collisions. Jozsó is among the authors of many other dAu papers, including a detailed analysis of centrality dependence of the nuclear modification factor in dAu collisions [3], the results of which will be used in our present theoretical analysis. The results of Ref. [4] about identified particle production and Ref. [5] about charge particle production will also be commented on.

Our group has performed theoretical investigations connected to the pp , dAu , and $AuAu$ collisions at RHIC energies in the framework of a RMKI-ELTE-Kent-Columbia collaboration. We would like to posthumously thank Jozsó with this paper on dAu collisions for his continuous interest in our work and for his support to keep our theoretical collaboration vital and successful in high-energy nuclear collision research.

^a e-mail: plevai@rmki.kfki.hu

2 Introduction

Recent experimental data on mid-rapidity π^0 production in the transverse momentum region $2 \text{ GeV}/c < p_T < 15 \text{ GeV}/c$ measured at the Relativistic Heavy Ion Collider (RHIC) in $AuAu$ collisions at $\sqrt{s} = 130 \text{ AGeV}$ and 200 AGeV display surprising evidence of new phenomena appearing in hot dense matter. Here we focus on the property that the π^0 transverse momentum spectrum shows a strong suppression [6–8] in central collisions compared to theoretical expectations based on binary collision dynamics in perturbative quantum chromodynamics (pQCD) calculations (see e.g. Refs. [9–11]). A similar suppression pattern was observed for charged hadrons [12]. Introducing final state interactions, especially jet energy loss [13–19], this suppression pattern can be reproduced both at 130 AGeV [20, 21] and 200 AGeV [22, 23]. The entanglement of initial and final state interactions in $AuAu$ collisions and the complexity of the theoretical calculation generated an increased interest in simpler reactions, such as the dAu collision. In this case final state interactions play a minor role, and the initial state interactions (initial multiscattering, shadowing) can be investigated cleanly. The obtained dAu data from RHIC [24–26] stimulated further interest in theoretical calculations of pion production in this reaction.

In a pQCD-based leading order (LO) parton model a systematic analysis of existing pA data has been completed [11] and our calculation will be based on results obtained there. A LO calculation of dAu was reported in Ref. [27]. Here we perform a dAu computation in next-to-leading order (NLO), utilizing recent developments for pp collisions [28]. Successful calculations based on the physics of gluon saturation have also been carried out for this system [29, 30].

In this paper we take advantage of the availability of detailed (impact-parameter selected) data and calculate the impact-parameter dependence of nuclear modification factor R_{dAu} in our pQCD based model.

The paper is organized as follows. In Section 2 we review the NLO pQCD-improved parton model augmented with the intrinsic transverse momentum distribution for pp collisions. We compare calculations to pp results at midrapidity at $\sqrt{s} = 200 \text{ GeV}$ and use these data to tune the parameters of the model. In Section 3, we discuss calculational details for the $d + Au \rightarrow \pi^0 + X$ reaction at $y = 0$ in the transverse momentum region $p_T > 2 \text{ GeV}/c$. In Section 4 the R_{dAu} nuclear modification factor is extracted from the data, and we investigate its impact parameter dependence. In particular, we study simple shadowing prescriptions without and with impact parameter dependence. In Section 5, we discuss our results.

3 The pQCD improved parton model with intrinsic k_T

The invariant cross section for neutral pion production in a pp collision can be described in the NLO pQCD-improved parton model on the basis of the factorization theorem as a convolution [28, 31, 32]:

$$E_\pi \frac{d\sigma^{pp}}{d^3p_\pi} = \frac{1}{S} \sum_{abc} \int_{VW/z_c}^{1-(1-V)/z_c} \frac{dv}{v(1-v)} \int_{VW/vz_c}^1 \frac{dw}{w} \int dz_c \int d^2\mathbf{k}_{Ta} \int d^2\mathbf{k}_{Tb} f_{a/p}(x_a, \mathbf{k}_{Ta}, Q^2) f_{b/p}(x_b, \mathbf{k}_{Tb}, Q^2) \cdot \left[\frac{d\tilde{\sigma}}{dv} \delta(1-w) + \frac{\alpha_s(Q_R)}{\pi} K_{ab,c}(s, v, w, Q, Q_R, Q_F) \right] \frac{D_c^\pi(z_c, Q_F^2)}{\pi z_c^2}, \quad (1)$$

where we use a product approximation for the parton distribution functions (PDFs),

$$f(x, \mathbf{k}_T, Q^2) = f(x, Q^2)g(\mathbf{k}_T). \quad (2)$$

Here, the function $f(x, Q^2)$ represents the standard NLO PDF as a function of momentum fraction x at factorization scale Q , $d\tilde{\sigma}/dv$ is the Born cross section of the partonic subprocess $ab \rightarrow cd$, $K_{ab,c}(s, v, w, Q, Q_R, Q_F)$ is the corresponding higher order correction term, and the

fragmentation function (FF), $D_c^\pi(z_c, Q_F^2)$, gives the probability for parton c to fragment into a pion with momentum fraction z_c at fragmentation scale Q_F . We use the conventional proton level (S, V, W) and parton level (s, v, w) kinematical variables of NLO calculations (see details in Refs. [28,31,32]). In our present study we consider fixed scales: the factorization and the renormalization scales are connected to the momentum of the intermediate jet, $Q = Q_R = \kappa \cdot p_q$ (where $p_q = p_T/z_c$), while the fragmentation scale is connected to the final hadron momentum, $Q_F = \kappa \cdot p_T$. The value of κ can be varied in a wide range, $\kappa \in [0.3, 3]$.

Our NLO calculation includes the initial transverse-momentum distribution $g(\mathbf{k}_T)$ of partons (“intrinsic k_T ”), along the lines of Refs. [9,11,28,33]. We demonstrated the success of such a treatment at LO level in Ref. [11]. In our phenomenological approach the transverse-momentum distribution is described by a Gaussian,

$$g(\mathbf{k}_T) = \frac{1}{\pi \langle k_T^2 \rangle} e^{-k_T^2 / \langle k_T^2 \rangle} . \quad (3)$$

Here, $\langle k_T^2 \rangle$ is the 2-dimensional width of the k_T distribution and it is related to the magnitude of the average transverse momentum of a parton as $\langle k_T^2 \rangle = 4 \langle k_T \rangle^2 / \pi$.

In our LO and NLO investigations we use GRV LO PDFs [34] and the MRST(cg) NLO PDFs [35] for parton distribution functions. For fragmentation functions we use the KKP parameterization [36], which has LO and NLO versions. An advantage of the GRV and the MRST sets is that they can be used down to very small scales ($Q^2 \approx 0.25 \text{ GeV}^2/c^2$). Thus, they provide reasonable calculations at relatively small transverse momenta, $p_T \geq 2 \text{ GeV}/c$ at our fix scales.

Figure 1 displays our LO and NLO pQCD results at $\sqrt{s} = 200 \text{ GeV}$ for $pp \rightarrow \pi^0 X$ [37] at different scales. In the LO case (dashed line) we used $\kappa = 2/3$ for both the factorization and the fragmentation scales to reproduce the data at high p_T within error bar. (This scale value is higher than $\kappa = 1/2$ used in Ref. [11] due to a readjustment triggered by the availability of precise data at high p_T on π^0 production in place of the earlier UA1 data on charged hadrons.) To minimize the difference between RHIC data and the model at low p_T a $\langle k_T^2 \rangle = 2.5 \text{ GeV}^2/c^2$ is included. We obtained quite good agreement in LO (see open squares in the data/pQCD ratio, lower panel).

In the NLO calculation we use the scales $Q = Q_R = (4/3)p_q$ and $Q_F = (4/3)p_T$ to reproduce the central value of the experimental data at high p_T (dash-dotted line in the upper panel). However, in the window $2 \text{ GeV}/c < p_T < 4 \text{ GeV}/c$ this choice underestimates the data by a factor of 2 (see filled triangles in the lower panel). These calculational results are in agreement with the calculation reported in Ref. [37], albeit with a different set of scales [38]. Since we plan to investigate multiscattering and the Cronin effect in dAu collisions, which are most pronounced in the above momentum window, we consider an NLO parameter set with scales $Q = Q_R = (4/3)p_q$ and $Q_F = (4/3)p_T$, together with an intrinsic k_T value $\langle k_T^2 \rangle = 2.5 \text{ GeV}^2/c^2$.

Fig. 1 indicates that we obtain good agreement both at high and low p_T with this choice (full line in the upper panel, filled squares in the lower panel). One can see that the results with this NLO parameter set and our LO results are close to each other, even though the scales differ by a factor 2. This is due to having the same width of the intrinsic k_T distribution. The physically realistic nature of the value found for the width is corroborated by results from di-jet production at lower energies: jet-jet correlations yield a similar value for $\langle k_T^2 \rangle$ at ISR energies [39]. While recent measurements of jet-jet correlations in pp collision at RHIC energies [40,41] may further clarify the properties of the transverse component of the PDFs, these parameterizations fixed in pp collisions will provide a solid basis to investigate nuclear collisions.

The precision of the NLO calculation at lower p_T could be improved introducing non-Gaussian or p_T -dependent intrinsic k_T (see e.g. Refs. [42,43]). In the present analysis we keep a constant value for the width of the Gaussian transverse momentum distribution in pp collisions. This way our results can be compared to the experimental data on measurable initial dijet transverse momentum in a simple way. This analysis has been accomplished [44], using recent data on di-hadron correlation [45]. The measured and theoretically extracted momentum imbalance value agrees very well with the one applied in our calculations.

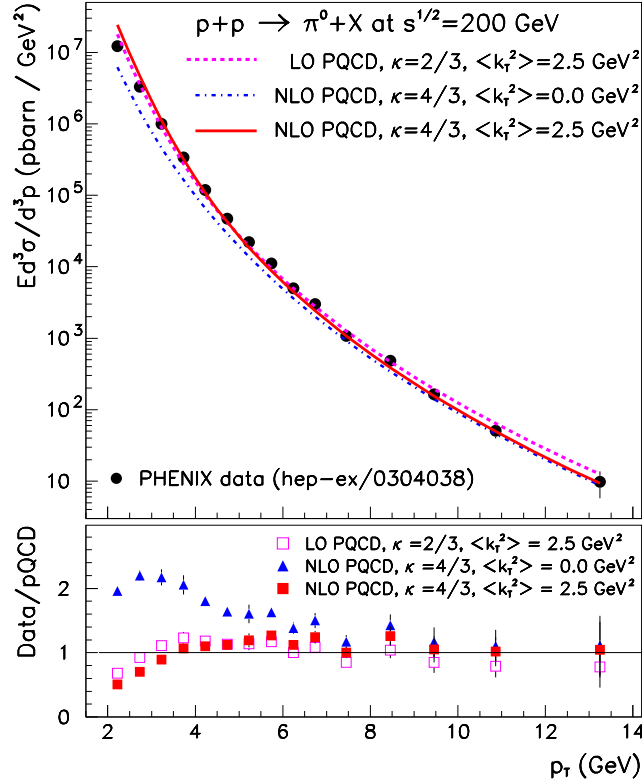


Fig. 1. Invariant cross section of pion production in $p + p \rightarrow \pi^0 + X$ at $\sqrt{s} = 200$ GeV. Upper panel displays spectra: LO result at scales $Q = (2/3)p_T/z_c$, $Q_F = (2/3)p_T$ and $\langle k_T^2 \rangle = 2.5$ GeV $^2/c^2$ (dashed line), NLO results at scales $Q = Q_R = (4/3)p_T/z_c$, $Q_F = (4/3)p_T$ without intrinsic k_T (dash-dotted line) and with $\langle k_T^2 \rangle = 2.5$ GeV $^2/c^2$ (solid line). Lower panel shows the data/pQCD ratios for LO (open squares), NLO without (triangles) and with (solid squares) intrinsic k_T at the above parameter values.

4 The parton model for dAu collisions

Considering the dAu collision, the hard pion production cross section can be written as an integral over impact parameter b , where the geometry of the collision is described in the Glauber picture:

$$E_\pi \frac{d\sigma_\pi^{dAu}}{d^3p} = \int d^2b d^2r t_d(r) t_{Au}(|\mathbf{b} - \mathbf{r}|) \cdot E_\pi \frac{d\sigma_\pi^{pp}(\langle k_T^2 \rangle_{pAu}, \langle k_T^2 \rangle_{pd})}{d^3p}, \quad (4)$$

where the proton-proton cross section on the right hand side represents the cross section from eq. (1), but with the broadened widths of the transverse-momentum distributions (3), as a consequence of nuclear multiscattering (see eq. (5)). Here $t_A(b) = \int dz \rho_A(b, z)$ is the nuclear thickness function (in terms of the density distribution of the gold nucleus, ρ_{Au}), normalized as $\int d^2b t_{Au}(b) = A_{Au} = 197$. For the deuteron, one could use a superposition of a pAu and a nAu collision, or a distribution for the nucleons inside the deuteron. For a first orientation we follow Ref. [27] in this regard, and apply a hard-sphere approximation for the deuteron with $A = 2$ for estimating the nuclear effects. Also, since π^0 production is not sensitive to isospin, we continue to use the notation “ pA ” when talking about the interaction of any nucleon with a nucleus.

The initial state broadening of the incoming parton distribution function is accounted for by an increase in the width of gaussian parton transverse momentum distribution in eq. (3):

$$\langle k_T^2 \rangle_{pA} = \langle k_T^2 \rangle_{pp} + C \cdot h_{pA}(b) . \quad (5)$$

Here, $\langle k_T^2 \rangle_{pp}$ is the width of the transverse momentum distribution of partons in pp collisions, $h_{pA}(b)$ describes the number of *effective* nucleon-nucleon (NN) collisions at impact parameter b , which impart an average transverse momentum squared C . The effectivity function $h_{pA}(b)$ can be written in terms of the number of collisions suffered by the incoming proton in the target nucleus, $h_{pA}(b) = \nu_A(b) - 1$. Here, $\nu_A(b) = \sigma_{NN} t_A(b)$, with σ_{NN} being the inelastic nucleon-nucleon cross section. Our preliminary results on the determination of the factor of C and $\nu(b)$ in an analysis in NLO confirm the findings of Ref. [11], where the systematic analysis of pA reactions was performed in LO and the characteristics of the Cronin effect were determined at LO level. Following Ref. [11], we assume that only a limited number of semi-hard collisions (with maximum $\nu_A(b)_{max} = 4$) contributes to the broadening, and the factor $C = 0.4 \text{ GeV}^2/c^2$. To give an indication of the dependence of the results on the value of C , we carried out a sample calculation with $C = 1 \text{ GeV}^2/c^2$.

At RHIC energies, parton broadening can be understood in terms of parton-level collisions. Elastic or small-angle-inelastic parton-parton collisions become responsible for the modification in the transverse momentum distribution, and this extra broadening will be superimposed to the original $\langle k_T^2 \rangle_{pp}$ value [10,46]. The above effectivity function, $h_{pA}(b)$, can be connected to the effective partonic collision length. In this framework formation time effects may result in a saturation-like behavior. In the following, we apply eq. (5) to describe the transverse momentum broadening of partons and use the above parameters.

It is well-known that the PDFs are modified in the nuclear environment. This is taken into account by various shadowing parameterizations [47–50]. In the present work, we display results obtained with the EKS parameterization, which has an antishadowing feature [48], and with the updated HIJING parameterization [47], which incorporates different quark and gluon shadowing, and has an impact-parameter dependent and an impact-parameter independent version. The impact-parameter dependence is taken into account by a term $\propto (1 - b^2/R_A^2)$, which re-weights the shadowing effect inside the nucleus.

The impact parameter dependence of the shadowing function can influence J/ψ production in dAu collisions in different rapidity windows [51]. The investigation of the centrality dependence of the pion production could contribute to the study of this interesting question.

5 Results on pion production in dAu collisions

Including the multiscattering and shadowing effects summarized in the previous section one can calculate the invariant cross section for pion production in dAu collision. Moreover, introducing the nuclear modification factor R_{dAu} , as

$$R_{dAu} = \frac{E_\pi d\sigma_\pi^{dAu}/d^3p}{N_{bin} \cdot E_\pi d\sigma_\pi^{pp}/d^3p} = \frac{E_\pi d\sigma_\pi^{dAu}(\text{ with nuclear effects})/d^3p}{E_\pi d\sigma_\pi^{dAu}(\text{ no nuclear effects})/d^3p} , \quad (6)$$

nuclear effects can be investigated clearly and efficiently, using a linear scale. The value of N_{bin} can be determined using the Glauber geometrical overlap integral as in eq. (4). Here we apply the right-most equation, which does not require the determination of N_{bin} from the Glauber model.

Figure 2 summarizes our results for the nuclear modification factor R_{dAu} in minimum bias dAu collisions at $\sqrt{s} = 200 \text{ AGeV}$. In the top panel the LO case with finite intrinsic k_T is displayed. The center panel shows the NLO case without intrinsic k_T in the pp collision, corresponding to a well-focused initial beam of partons, but including the nuclear broadening effect connected to multiscattering. The bottom panel shows the NLO results with initial intrinsic k_T in the pp collision and nuclear broadening.

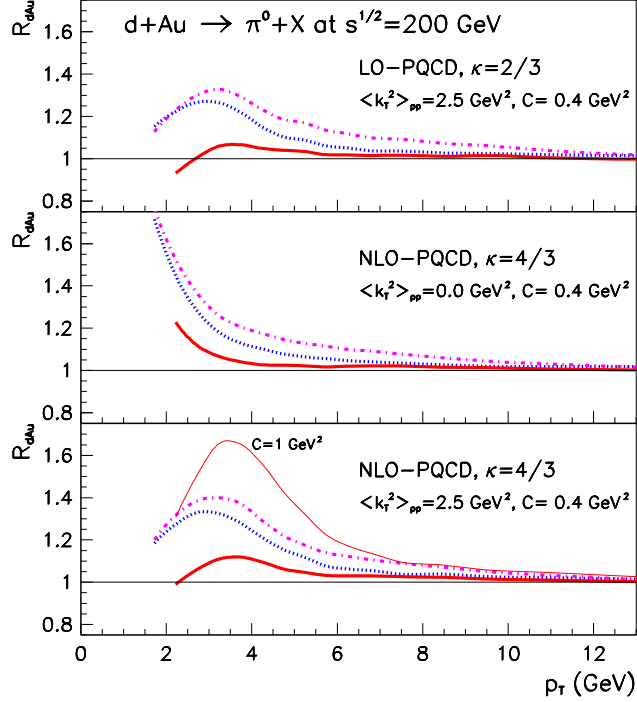


Fig. 2. The R_{dAu} nuclear modification factor for minimum bias dAu collision in LO (upper panel), in NLO without (middle panel) and with (lower panel) intrinsic k_T . For details see text and Fig. 1. The dotted lines indicate the enhancement in R_{dAu} connected to multiscattering only, which is characterized by the average broadening per NN collision, $C = 0.4 \text{ GeV}^2/c^2$. Thick solid lines show the results after additionally including a b -independent shadowing parameterization from the HIJING model [47]. The thin line in the bottom panel was obtained with $C = 1 \text{ GeV}^2/c^2$. The dash-dotted lines display the influence of the EKS-shadowing [48], which has an anti-shadowing contribution, increasing R_{dAu} .

The dashed lines indicate the Cronin enhancement connected to the nuclear multiscattering characterized by $C = 0.4 \text{ GeV}^2/c^2$. The peak structure with an enhancement of 25% is clearly seen in the case of large initial intrinsic k_T (top and bottom panels), but in the middle panel the Cronin peak is shifted to too small values of p_T , out of the range of our pQCD calculations (this property was discussed in Ref. [52]).

The influence of shadowing is indicated by thick solid lines in Fig. 2: a relative decrease of R_{dAu} is obtained using a b -independent parameterization of shadowing applied in the HIJING model [47]. Altogether, an upto 10% enhancement can be seen in the $3 \text{ GeV}/c < p_T < 5 \text{ GeV}/c$ region, which disappears at higher p_T . The height of the peak depends on the value of the multiscattering parameter C at a fixed shadowing parameterization. To illustrate this, we included a calculation with $C = 1 \text{ GeV}^2/c^2$ in the bottom panel of Fig. 2 (thin line). The position of the peak is related to the intrinsic k_T value in the pp collision: smaller value leads to a shift to smaller p_T [52]. The EKS parameterization [48], which contains anti-shadowing, leads to a small surplus in R_{dAu} , as expected (dash-dotted lines).

Figure 3 displays the centrality dependence of our NLO results ($\kappa = 4/3$, $\langle k_T^2 \rangle_{pp} = 2.5 \text{ GeV}^2/c^2$, $C = 0.4 \text{ GeV}^2/c^2$) for the nuclear modification factor R_{dAu} with the HIJING shadowing [47]. The left column shows the b -independent cases. Here, the central bins (upper panel) yield essentially overlapping results, because both, multiscattering and shadowing depend on the length of the target matter (approximately constant in these cases). Shadowing finally wins moving toward peripheral collisions (lower panel), because the Cronin effect disappears with

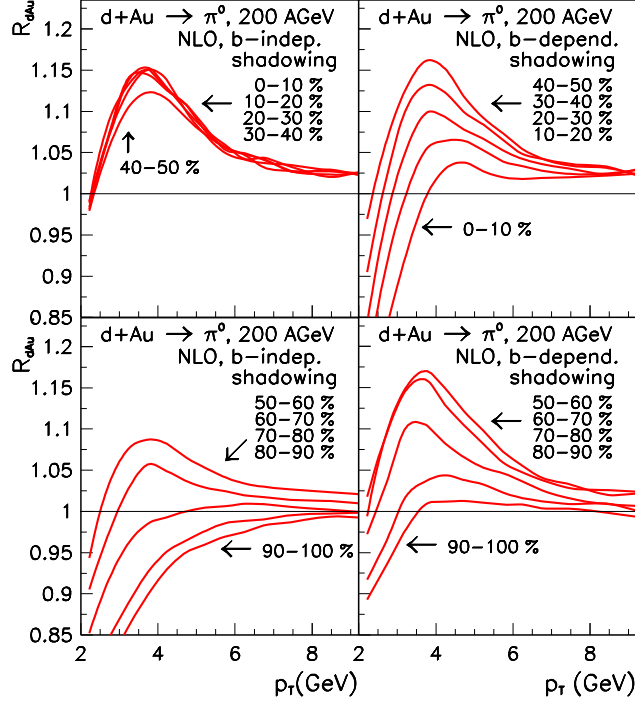


Fig. 3. The impact parameter dependence of the nuclear modification factor R_{dAu} for b -independent shadowing (right column) and b -dependent shadowing (left column). The lines correspond to different centrality bins with an increment of 10%. The 5 “central” curves (0-50%) are shown in the upper panels, and the remaining 5 (“peripheral”) cases (50-100%) can be seen in the lower panels.

decreasing $\nu_A(b)$, but a slight shadowing is generated even in the most peripheral cases in the recent parameterization of Ref. [47]. However, there is a strong suppression in central collisions in the b -dependent parameterization, which is not balanced by the Cronin effect (see upper right panel). Shadowing is rapidly decreasing in this parameterization at larger impact parameter (bottom right panel), and the Cronin effect becomes dominant for a certain b -range, increasing the nuclear modification factor. Finally, in peripheral collisions the Cronin effect vanishes, and in lack of strong shadowing the nuclear modification factor recovers to unity at a reasonable transverse momentum value. Precise data on the centrality dependence in the nuclear modification factor could yield information about the interplay between multiscattering (including saturated vs. non-saturated parameterizations of multiscattering) and shadowing in the dAu collision.

Figure 4 is constructed to emphasize the structure and properties of Fig. 3. The centrality dependence of R_{dAu} is shown at fix $p_T = 3.7$ GeV/c, in the peak region of R_{dAu} . It is easy to appreciate the difference between the b -independent (solid line) and the b -dependent shadowing (dashed line) from this Figure.

Figure 5 (top panel) displays our results for the nuclear modification factor in minimum bias dAu collision for b -independent and b -dependent shadowing parameterizations from HIJING. Here we have $\kappa = 4/3$ for the scales in the NLO calculation, and we use $\langle k_T^2 \rangle_{pp} = 2.5$ GeV²/c² and $C = 0.4$ GeV²/c², as in the bottom panel of Fig. 2. In spite of the very different impact parameter dependence of R_{dAu} the minimum bias results are very close to each other. This is because many details are averaged out in minimum bias data, and the final result is no longer sensitive to the b -dependence of shadowing. These results can be directly compared to the minimum bias experimental data. In h^\pm minimum bias data we expect a larger enhancement in

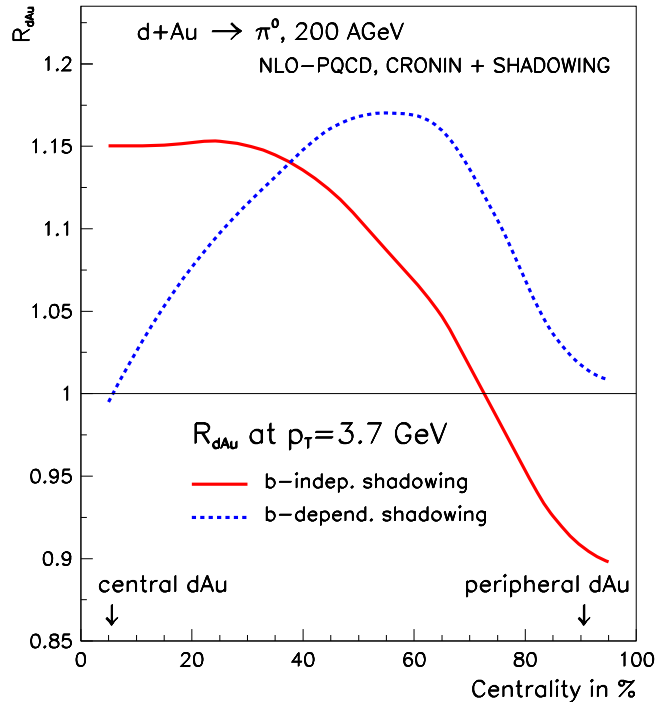


Fig. 4. The centrality dependence of the nuclear modification factor R_{dAu} in the peak region, at fix $p_T = 3.7$ GeV/c. The solid line corresponds to the case of b -independent shadowing, the dashed line describes b -dependent shadowing.

the nuclear modification factor at this energy, due to the presence of protons and antiprotons, which are known to yield anomalous p/π ratios [53]. Uncertainties in the treatment of fragmentation into protons [54] preclude a detailed prediction of R_{dAu} for h^\pm at the present time. On the other hand, parton fragmentation may overlap with parton coalescence in the intermediate transverse momentum range, as it was investigated in $AuAu$ collisions [55–57], and this effect may have influence in dAu collisions.

In the bottom panel of Figure 5 we display the double ratio of the nuclear modification factors for central to peripheral collision, $R^* = R_{dAu}(0 - 50\%) / R_{dAu}(50 - 90\%)$. The full line indicates the ratio R^* for the b -independent shadowing and the dashed line corresponds to the b -dependent shadowing. In the window $2 \text{ GeV}/c < p_T < 3 \text{ GeV}/c$ the obtained difference is $\sim 30\%$, which could be seen in case of high precision data are available.

Figure 6 displays recent high precision experimental data at different centralities on pion production in dAu collisions at $\sqrt{s_{NN}} = 200$ GeV [3]. We applied our model and calculated pion production, including HIJING shadowing (solid lines) and EKS shadowing (dash-dotted lines). Although the size of the error bars does not allow us to draw a firm conclusion about centrality dependence, selecting transverse momentum windows at $p_T \approx 3.7$ GeV/c, we may see a tendency similar to the dashed line in Fig. 4. However, in a recent paper [58], applying the HKM shadowing function, we investigated in detail the most central dAu data and have found an indication of the presence of jet energy loss in cold matter. This finding means that theoretical descriptions have to deal with nuclear shadowing, multiscattering, and jet energy loss already in dAu collisions, and may possibly lead to a structure similar to the full line in Fig. 4. This interplay can be investigated quantitatively if the precision of the data will become even higher by the analysis of a forthcoming dAu run.

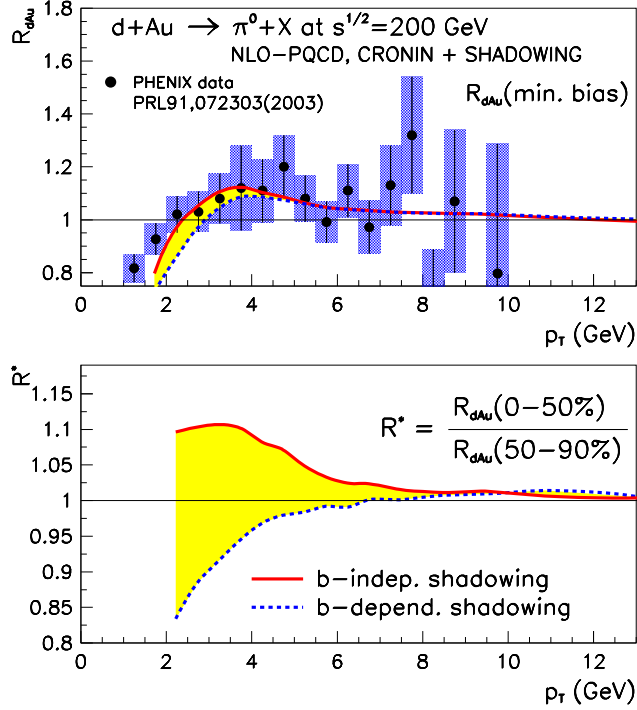


Fig. 5. Top panel: the nuclear modification factor R_{dAu} for minimum bias dAu collisions obtained from our NLO calculation in case of b -independent (solid line) and b -dependent shadowing (dashed line). Experimental data are from the PHENIX Collaboration [24]. Bottom panel: the double ratio of the nuclear modification factors for central to peripheral collision, $R^* = R_{dAu}(0-50\%)/R_{dAu}(50-90\%)$. The full line indicates the ratio R^* for the b -independent shadowing, the dashed line corresponds to the b -dependent shadowing.

6 Discussion

Summarizing our theoretical results in a NLO pQCD-based parton model calculation for the dAu collision, we see a clear enhancement ($\approx 10 - 15\%$) in the nuclear modification factor R_{dAu} after including nuclear multiscattering and HIJING shadowing. Our NLO calculation of pion production in the dAu collision confirms earlier LO results, while providing an updated description of the invariant cross section and the interplay between multiscattering and shadowing effects. We have found that there is a qualitative difference between position-independent and position-dependent shadowing; the specific structure of the centrality dependence of the nuclear modification factor results in maximum enhancement in semi-central collisions for position-dependent shadowing. Thus, the centrality dependence of R_{dAu} may be used to obtain detailed information about the effects of multiscattering and shadowing.

Recent experimental data on π^0 production [3] allow us to perform a detailed investigation of centrality dependence. Although the minimum bias π^0 data display a 10-15% increase in the nuclear modification factor supporting the idea of interplay between multiscattering and shadowing in the reproduction of the Cronin effect, but detailed conclusion can not be obtained at the recent precision of the data. The h^\pm data [4,5] appear to have an even larger increase, but we do not have a theory comparison for these data at present, because the proton (and antiproton) production is not well described by recent pQCD based parton models.

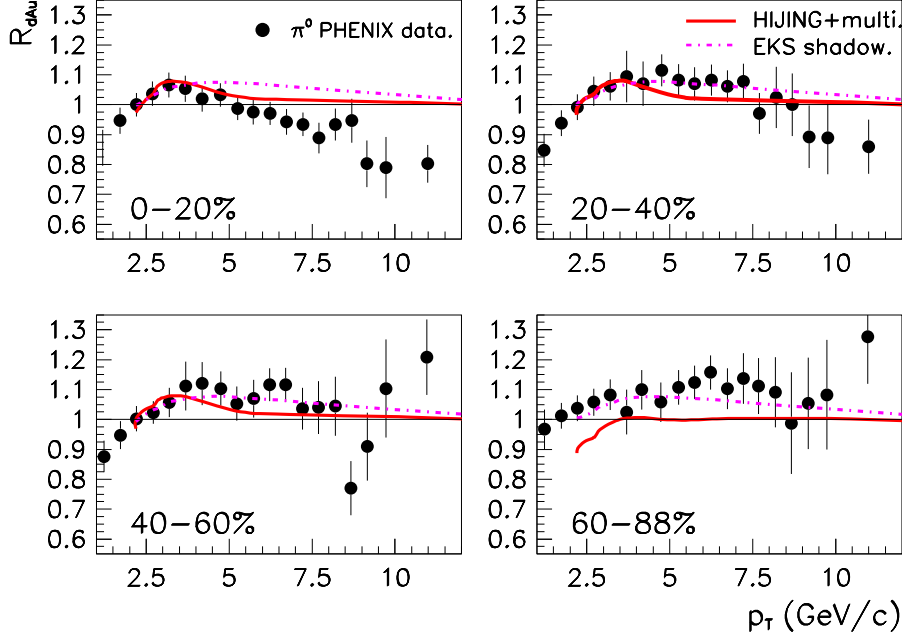


Fig. 6. The nuclear modification factor R_{dAu} for pion production in dAu collisions at different centralities measured by PHENIX Collaboration [3]. Results from our NLO calculation are displayed with b -independent HIJING shadowing (solid line). Dashed line corresponds to b -independent EKS shadowing.

Acknowledgments: We thank G. David, M. Gyulassy, I. Vitev, and X.N. Wang for useful comments and stimulating discussions. We are grateful to P. Aurenche and his collaborators for their NLO code, which served as the basis of calculational developments reported here. This work was supported in part by U.S. DOE grants DE-FG02-86ER40251, DE-FG02-93ER40764, MTA-OTKA-NSF grant INT-0000211 and Hungarian grants T034842, T043455, NK062044, IN71374. Supercomputer time provided by BCPL in Norway and the EC – Access to Research Infrastructure action of the Improving Human Potential programme is gratefully acknowledged.

References

1. S.A. Bass, ..., J. Zimányi, ..., Nucl. Phys. **A661**, (1999) 205.
2. S.S. Adler *et al.* (PHENIX Coll.), Phys. Rev. Lett. **91**, (2003) 072303.
3. S.S. Adler *et al.* (PHENIX Coll.), Phys. Rev. Lett. **98**, (2003) 172302.
4. S.S. Adler *et al.* (PHENIX Coll.), Phys. Rev. **C74**, (2006) 024904.
5. S.S. Adler *et al.* (PHENIX Coll.), [arXiv: 0708.2416](https://arxiv.org/abs/0708.2416) [nucl-ex].
6. G. David *et al.* (PHENIX Coll.), Nucl. Phys. **A698**, (2002) 227; K. Adcox *et al.* (PHENIX Coll.), Phys. Rev. Lett. **88**, (2002) 022301; K. Adcox *et al.* (PHENIX Coll.), Phys. Lett. **B561**, (2003) 82.
7. S. Mioduszewski *et al.* (PHENIX Coll.), Nucl. Phys. **A715**, (2003) 453c; D. d’Enterria *et al.* (PHENIX Coll.), Nucl. Phys. **A715**, (2003) 749c.
8. C. Adler *et al.* (STAR Coll.), Phys. Rev. Lett. **89**, (2002) 202301; J. Adams *et al.* (STAR Coll.), Phys. Rev. Lett. **91**, (2003) 172302.
9. X.N. Wang, Phys. Rev. **C61**, (2001) 064910.
10. G. Papp, G.G. Barnaföldi, G. Fai, P. Lévai, and Y. Zhang, Nucl. Phys. **A698**, (2002) 627.

11. Y. Zhang, G. Fai, G. Papp, G.G. Barnaföldi, and P. Lévai, Phys. Rev. **C65**, (2002) 034903.
12. J.L. Klay *et al.*, (STAR Coll.), Nucl. Phys. **A715**, (2003) 733c; G.J. Kunde *et al.* (STAR Coll.), Nucl. Phys. **A715**, (2003) 189c.
13. M. Gyulassy and M. Plümer, Phys. Lett. **B243**, (1990) 432;
M. Gyulassy, M. Plümer, M.H. Thoma and X.-N. Wang, Nucl. Phys. **A538**, (1992) 37c.
14. X.-N. Wang and M. Gyulassy, Phys. Rev. Lett. **68**, (1992) 1480.
15. M. Gyulassy, P. Lévai, and I. Vitev, Phys. Rev. Lett. **85**, (2000) 5535; Nucl. Phys. **B571**, (2000) 197; *ibid.* **B594**, (2001) 371.
16. R. Baier, Y.L. Dokshitzer, A.H. Mueller, S. Peigné, and D. Schiff, Nucl. Phys. **B483**, (1997) 291; *ibid.* **B484**, (1997) 265. R. Baier, D. Schiff and B.G. Zakharov, Ann. Rev. Nucl. Part. Sci. **50**, (2000) 37.
17. B.G. Zakharov, JETP Lett. **70**, (1999) 176; *ibid.* **73**, (2001) 49; *ibid.* **80**, (2004) 67; *ibid.* **80**, (2004) 617.
18. U.A. Wiedemann, Nucl. Phys. **A690**, (2001) 731.
19. M. Gyulassy, P. Lévai, and I. Vitev, Phys. Lett. **B538**, (2002) 282.
20. P. Lévai, G. Papp, G. Fai, M. Gyulassy, G.G. Barnaföldi, I. Vitev, and Y. Zhang, Nucl. Phys. **A698**, (2002) 631.
21. X.N. Wang, Nucl. Phys. **A698**, (2002) 296.
22. X.N. Wang, Phys. Lett. **B595**, (2004) 165.
23. G.G. Barnaföldi, P. Lévai, G. Papp, G. Fai, and M. Gyulassy, Eur. Phys. J. **C33**, (2004) S609.
24. S.S. Adler *et al.* (PHENIX Coll.) Phys. Rev. Lett. **91**, (2003) 072303.
25. B.B. Back *et al.* (PHOBOS Coll.) Phys. Rev. Lett. **91**, (2003) 072302.
26. J. Adams *et al.* (STAR Coll.) Phys. Rev. Lett. **91**, (2003) 072304.
27. I. Vitev, Phys. Lett. **B562**, (2003) 36.
28. G. Papp, G.G. Barnaföldi, P. Lévai, and G. Fai, hep-ph/0212249.
29. D. Kharzeev, Yu.V. Kovchegov, and K. Tuchin Phys. Rev. **D68**, (2003) 094013; Phys. Lett. **B599**, (2004) 23.
30. E. Iancu, R. Itakura, and D.N. Triantafyllopoulos, Nucl. Phys. **A742**, (2004) 182.
31. F. Aversa, P. Chiappetta, M. Greco, and J.Ph. Guillet, Nucl. Phys. **B327**, (1989) 105.
32. P. Aurenche, M. Fontannaz, J.Ph. Guillet, B. Kniehl, E. Pilon, and M. Werlen, Eur. Phys. J. **C9**, (1999) 107; P. Aurenche, M. Fontannaz, J.Ph. Guillet, B. Kniehl, and M. Werlen, Eur. Phys. J. **C13**, (2001) 347.
33. C.Y. Wong and H. Wang, Phys. Rev. **C58**, (1998) 376.
34. M. Gluck, E. Reya, and A. Vogt, Z. Phys. **C67**, (1995) 433.
35. A.D. Martin, R.G. Roberts, W.J. Stirling, and R.S. Thorne, Eur. Phys. J. **C23**, (2002) 73.
36. B.A. Kniehl, G. Kramer, and B. Pötter, Nucl. Phys. **B597**, (2001) 337;
37. H. Torii *et al.* (PHENIX Coll.), Nucl. Phys. **A715**, (2003) 753c; S.S. Adler *et al.* (PHENIX Coll.), Phys. Rev. Lett. **91**, (2003) 241803.
38. In the NLO calculation displayed in Fig. 2c of Ref. [37], the scale choice $Q = Q_R = Q_F = p_T$ appears to be a good general fit within error bars; however, concentrating on the central values at high p_T would prefer scales like $Q = Q_R = Q_F = (5/3)p_T$, leading to a factor 2 underestimation of the data at low p_T , just like in our calculation.
39. A.L.S. Angelis, *et al.* (CCOR Coll.), Phys. Lett. **B97**, (1980) 163.
40. C. Adler *et al.* (STAR Coll.), Phys. Rev. Lett. **90**, (2003) 082302; D. Hardtke *et al.* (STAR Coll.), Nucl. Phys. **A715**, (2003) 801c.
41. M. Chiu *et al.* (PHENIX Coll.), Nucl. Phys. **A715**, (2003) 761c; N.N. Ajitanand *et al.* (PHENIX Coll.), Nucl. Phys. **A715**, (2003) 765c.
42. M. Gyulassy, P. Lévai, and I. Vitev, Phys. Rev. **D66**, (2002) 014005.
43. A. Gawron, J. Kwiecinski, and W. Broniowski, Phys. Rev. **D68**, (2003) 054001.
44. P. Lévai, G. Fai, G. Papp, Phys. Lett. **B634**, (2006) 383; G. Fai, P. Lévai, G. Papp, Nucl. Phys. **A774**, (2006) 557; *ibid.* **A783**, (2007) 535.
45. S.S. Adler *et al.*, Phys. Rev. **D74**, (2006) 072002.
46. A. Accardi, Eur. Phys. J. **C43**, (2005) 121.
47. S.J. Li and X.N. Wang, Phys. Lett. **B527**, (2002) 85.
48. K.J. Eskola, V.J. Kolhinen, and C.A. Salgado, Eur. Phys. J. **C9**, (1999) 61.
49. M. Hirai, S. Kumano, and M. Miyama, Phys. Rev. **D64**, (2001) 034003; M. Hirai, S. Kumano, and T.H. Nagai, Phys. Rev. **C70**, (2004) 044905.
50. L. Frankfurt, V. Guzey, M. McDermott, and M. Strikman, JHEP **02**, (2002) 027.
51. S.R. Klein, R. Vogt, Phys. Rev. Lett. **91**, (2004) 142301; R. Vogt, hep-ph/0405060.

52. G.G. Barnaföldi, P. Lévai, G. Papp, G. Fai, and Y. Zhang, [nucl-th/0212111](#).
53. K. Adcox *et al.* (PHENIX Coll.), *Phys. Rev. Lett.* **88**, (2002) 242301;
T. Chujo *et al.* (PHENIX Coll.), *Nucl. Phys.* **A715**, (2003) 151c;
T. Sakaguchi *et al.* (PHENIX Coll.), *Nucl. Phys.* **A715**, (2003) 757c;
T. Chujo *et al.* (PHENIX Coll.), *J. Phys.* **G34**, (2007) S893.
54. X. Zhang, G. Fai, and P. Lévai, *Phys. Rev. Lett.* **89**, (2002) 272301.
55. R.C. Hwa, C.B. Yang, *Phys. Rev.* **C67**, (2003) 034902.
56. V. Greco, C.M. Ko, and P. Lévai, *Phys. Rev. Lett.* **90**, (2003) 202302; *Phys. Rev.* **C68**, (2003) 034904.
57. R.J. Fries, B. Müller, C. Nonaka, and S.A. Bass, *Phys. Rev. Lett.* **90**, (2003) 202303; *Phys. Rev.* **C68**, (2003) 044902.
58. B.A. Cole, G.G. Barnaföldi, P. Lévai, G. Papp, and G. Fai, [hep-ph/0702101](#).